





## Synthesis and Characterization of Carbonate-Substituted Hydroxyapatite from Eggshell Waste Using Urea and Diammonium Hydrogen Phosphate



Raihan Annisa Fitri<sup>1</sup>, Arief Wirakusuma<sup>1</sup>, Muhammad Prayogie Aulia<sup>1,2</sup>, Ratni Dewi<sup>3</sup>,  
Nasrul Arahman<sup>1,4,5\*</sup>

<sup>1</sup> Department of Chemical Engineering, Universitas Syiah Kuala, Banda Aceh 23111, Indonesia

<sup>2</sup> Department of Chemical Engineering, Kobe University, Kobe 657-8501, Japan

<sup>3</sup> Department of Chemical Engineering, Lhokseumawe State Polytechnic, Lhokseumawe 24301, Indonesia

<sup>4</sup> Research Center for Environmental and Natural Resources, Universitas Syiah Kuala, Banda Aceh 23111, Indonesia

<sup>5</sup> School of Environmental Management, Universitas Syiah Kuala, Banda Aceh 23111, Indonesia

Corresponding Author Email: [Nasrular@usk.ac.id](mailto:Nasrular@usk.ac.id)

Copyright: ©2024 The authors. This article is published by IETA and is licensed under the CC BY 4.0 license (<http://creativecommons.org/licenses/by/4.0/>).

<https://doi.org/10.18280/acsm.480612>

### ABSTRACT

**Received:** 7 August 2024

**Revised:** 3 November 2024

**Accepted:** 4 December 2024

**Available online:** 31 December 2024

#### Keywords:

calcium, eggshells, hydroxyapatite (HAp), phosphate, urea

Hydroxyapatite (HAp) is widely recognized for its application in medical implants, specifically as a bone substitute due to its biocompatibility. This study explores the synthesis of HAp using calcium oxide sourced from calcined eggshell waste treated with acetic acid. The focus is on evaluating the impact of varying concentrations of diammonium hydrogen phosphate ((NH<sub>4</sub>)<sub>2</sub>HPO<sub>4</sub>) and urea (CH<sub>4</sub>N<sub>2</sub>O) on the characteristics of carbonate-substituted hydroxyapatite. Calcining the eggshell waste at 900°C produced calcium oxide with a high yield of 89.3 wt.% CaO. This CaO was subsequently utilized in reactions with (NH<sub>4</sub>)<sub>2</sub>HPO<sub>4</sub> and urea to produce HAp. The introduction of (NH<sub>4</sub>)<sub>2</sub>HPO<sub>4</sub> not only contributed to the phosphate content but also influenced the crystalline structure and visual properties, such as brightness, of the final HAp product. Fourier-transform infrared (FTIR) analysis identified functional groups including hydroxyl (OH<sup>-</sup>), phosphate (PO<sub>4</sub><sup>3-</sup>), and carbonate (CO<sub>3</sub><sup>2-</sup>). Scanning electron microscopy (SEM) revealed that the synthesized HAp exhibited a granular morphology with particles ranging in size from 111.7 to 189.8 nm. The study determined a calcium-to-phosphorus (Ca/P) ratio of 1.59, demonstrating the feasibility of using eggshell waste as a sustainable source for high-quality HAp production.

## 1. INTRODUCTION

Hydroxyapatite (HAp) is widely recognized and extensively utilized in biomedical and bone tissue engineering due to its numerous benefits [1]. This white hexagonal solid exhibits a high affinity for heavy metal ions, making it valuable as an adsorbent for environmental protection purposes [2]. The impact and function of HAp particles are significantly influenced by their composition, size, and morphology. Spherical HAp particles possess a greater specific surface area and better fluidity than other HAp types, showing potential for surface adsorption and protein purification [3].

Among the HAp synthesis techniques, the wet precipitation method involves preparing two solutions: acidic and alkaline. The HAp precipitation is achieved by gradually adding the acidic solution to the alkaline solution. Following this, the HAp undergoes filtration, drying, and heat treatment. This method offers advantages such as low reaction temperatures, precise chemical composition control, and microstructural features management. Additionally, precipitation can produce nanosized HAp crystals at low temperatures and relatively low cost [4]. The structure and chemical composition of HAp can be altered by adjusting factors like reaction time, reaction

temperature, concentration, type of reagent, and drying and heat treatment conditions. Modifying the temperature during wet-method synthesis may affect parameters like crystallite size and degree of crystallinity, potentially influencing the biocompatibility of HAp [5].

In recent decades, HAp synthesis using natural sources has gained favor because HAp shares the same chemical composition as human bone, unlike synthetic materials [6]. Natural sources of HAp include bovine and human bones, fish bones and shells, snail shells, eggshells, oyster shells, corals, leaves, plant stalks (such as mint, basil, trifolium, and green tea), and algae. Many of these natural resources are low-cost wastes and readily available. Research on using waste materials to prepare HAp and other biocompatible materials has significantly increased in recent years, as it offers the dual benefits of repurposing waste into valuable products and reducing harmful environmental waste [2]. One auspicious source is chicken eggshells, which have a high calcium content (carboxylate is an essential component in HAp production), significant environmental impact, and readily accessible components [7].

HAp development has been extensively reported in previous studies, and various synthesis routes have been

developed to produce HAp from eggshell biogenic waste materials. Wanniarachchi et al. [8] produced HAp from eggshells using phosphoric acid and ammonium hydroxide, converting the resulting HAp into hexagonal  $\beta$ -tricalcium phosphate ( $\beta$ -TCP). Gintu et al. [9] synthesized HAp from laying hen eggshells by precipitation using monopotassium phosphate and ammonia, achieving a yield of 77.75%. Wu et al. [10] successfully synthesized HAp through a hydrothermal process and precipitation, finding the hydrothermal method effective and convenient for large-scale production. Azis et al. [11] utilized the sol-gel method to synthesize HAp from chicken eggshells via calcination, hydration, and carbonation. The development of HAp using other materials has been reported in previous studies, including calcium nitrate, calcium hydroxide, and calcium sulfate [12-14]. Compared to these approaches, our study introduces a synthesis method involving urea and  $(\text{NH}_4)_2\text{HPO}_4$  as precursors, with the aim of optimizing the conditions for creating an ideal suspension and enhancing the structural and functional characteristics of HAp.

This experimental approach is unprecedented, particularly in the utilization of eggshell waste as a raw material and as a potential solution for waste management. Consequently, the most recent information regarding the integration of urea and  $(\text{NH}_4)_2\text{HPO}_4$  represents significant data for further development. Additionally, this investigation aimed to evaluate the resultant HAp in terms of its morphology, functional groups, elemental composition, crystallinity, crystal size, and thermal behavior.

## 2. EXPERIMENTAL DETAILS

### 2.1 Materials

The chicken eggshell waste used in this study was obtained from small home-based industries around Banda Aceh, Indonesia. Acetic acid ( $\text{CH}_3\text{COOH}$ ), diammonium hydrogen phosphate ( $(\text{NH}_4)_2\text{HPO}_4$ ), and urea ( $\text{CH}_4\text{N}_2\text{O}$ ) were purchased from Sigma Aldrich. Distilled water (DI) was obtained from the Environmental Testing Engineering Laboratory, Universitas Syiah Kuala.

### 2.2 Synthesis of calcium oxide from eggshells

The chicken eggshell waste was washed several times using distilled water and then boiled for 15 minutes to remove impurities. The eggshells were then dried in an oven at  $110^\circ\text{C}$  for 2 hours until the moisture content was eliminated and their weight was constant. Subsequently, the dried eggshells underwent a calcination process at  $900^\circ\text{C}$  in a furnace for 2 hours to form calcium oxide (CaO). The obtained CaO was then characterized using X-ray fluorescence spectrometry (XRF).

### 2.3 Preparation of calcium acetate, $(\text{NH}_4)_2\text{HPO}_4$ , and urea solutions

The resulting CaO powder (2.8 grams) was added to an Erlenmeyer flask containing 50 ml of 2 M acetic acid. The suspension was stirred at 300 rpm and heated to  $50^\circ\text{C}$  until the solid CaO dissolved. The obtained solution was filtered before further use in synthesizing HAp. A 0.5 M  $(\text{NH}_4)_2\text{HPO}_4$  solution was prepared by dissolving 3.3 g of  $(\text{NH}_4)_2\text{HPO}_4$  in 50 ml of distilled water, whereas different concentrations of

urea solutions were prepared by dissolving 3 g of urea in 50 ml of distilled water to make 1 M, 1.5 M, and 2 M solutions, respectively.

### 2.4 Synthesis of HAp

A 1:1:1 mixture (based on volume ratio) of CaO filtrate,  $(\text{NH}_4)_2\text{HPO}_4$ , and urea was added to an Erlenmeyer flask and stirred at 300 rpm until homogeneous. The  $\text{NH}_4\text{OH}$  solution was slowly added to the flask until it reached a pH of 9. The solution was then allowed to stand for 24 hours at room temperature to precipitate HAp at the bottom of the flask. The precipitate was subsequently filtered and dried in an oven at  $90^\circ\text{C}$  for two hours.

### 2.5 Characterizations of HAp

The CaO content of the calcined eggshells was analyzed using XRF (PanAnalytical Serie Axios, Philips, UK) at 50 kV and 40 mA with a 10-minute acquisition time. A total of 0.5 g of sample was weighed, and the ratio of flux chemical used was ten times the sample weight. The glass beads used had a diameter of 32 mm. Platinum crucibles were used for sample preparation with lithium bromide as the solvent. The HAp functional groups were identified using Fourier-transform infrared spectroscopy (FTIR) (Shidmazu IR Prestige-21, Japan) in the range of  $4000\text{--}400\text{ cm}^{-1}$  with a resolution of  $4\text{ cm}^{-1}$  and 64 scans per acquisition with a KBr pellet method. The measurements were conducted at wavelengths between  $400\text{--}4000\text{ cm}^{-1}$ . The structure of HAp and its degree of crystallization were analyzed by X-ray diffraction (XRD) (Shidmazu XRD-6000, Japan) with  $\text{Cu-K}\alpha$  radiation ( $\lambda = 1.5406\text{ \AA}$ ) at 40 kV and 30 mA. The HAp diffraction pattern was measured  $2\theta$  between  $5^\circ$  and  $70^\circ$  at a rate of  $2^\circ/\text{minute}$  and compared with the ICDD (International Center for Diffraction Data) standard material data. The change in HAp enthalpy as a function of temperature was measured using differential scanning calorimetry (DSC) (Shidmazu, DSC/TGA-60, Japan). A 15-25 mg sample was placed in alumina crucibles and heated from  $50\text{--}1100^\circ\text{C}$  at  $10^\circ\text{C}/\text{min}$  under an argon gas atmosphere. The surface morphology of HAp was observed using scanning electron microscopy (SEM) with energy-dispersive X-ray spectroscopy (EDX) (Carl Zeiss-Bruker, Type EVO MA10, Germany). The instrument was operated at 3 kV and 50 kV. For the EDX measurements, the specimen was coated with gold to increase the contrast between the observed specimen and the surrounding environment.

## 3. RESULTS AND DISCUSSION

### 3.1 Chemical composition of calcinated eggshells

The purity of raw materials in the synthesis process of a material is crucial. The synthesis of hydroxyapatite (HAp) requires calcium acetate ( $(\text{CH}_3\text{COO})_2\text{Ca}$ ) as a source to react with  $(\text{NH}_4)_2\text{HPO}_4$  and urea, resulting in the precipitation of HAp. Calcium acetate can be obtained from the reaction between CaO and acetic acid. In this process, the purity of CaO is essential, as it influences the purity and yield of HAp. CaO itself is derived from the calcination of  $\text{CaCO}_3$  in eggshell waste, making the initial treatment of the raw material critical. Table 1 shows the characterization results of the calcined eggshells (CaO) obtained after the calcination of  $\text{CaCO}_3$  using

XRF analysis. The chemical composition of the calcined eggshells is dominated by CaO, indicating that the primary constituent is CaO. The chemical composition of CaO in the calcined eggshells is 89.3 wt%, with other impurities below 0.5 wt%. This high content will positively impact the HAp synthesis process, as the resulting calcium acetate will also be purer. Khalid et al. [15] reported experiments on calcining CaCO<sub>3</sub> to produce CaO, confirming that calcination temperatures of 900-1100°C can convert CaCO<sub>3</sub> to CaO. In another study, Razak et al. [16] also reported on the formation of CaO from the calcination of CaCO<sub>3</sub>. They found that different calcination temperatures, such as 700, 800, and 900°C, resulted in different CaO particle sizes, with 900°C producing the smallest particles and optimal results. The smaller particle size at 900°C increases the surface area and reactivity of CaO, which can improve the efficiency of the subsequent HAp synthesis by enhancing the reaction between calcium acetate, (NH<sub>4</sub>)<sub>2</sub>HPO<sub>4</sub>, and urea. Higher temperatures also promote higher purity CaO by more effectively driving off CO<sub>2</sub> during the calcination process. Additionally, Eze et al. [17] reported that their XRF analysis showed that the concentration of CaO obtained from the calcination process was around 90 wt%. Thus, the CaO produced in this study (89.3 wt%) is consistent with the results of other CaCO<sub>3</sub> calcination processes reported in the literature, and the high purity and small particle size of CaO at optimal calcination temperatures will likely enhance the HAp synthesis process.

**Table 1.** Chemical composition by XRF of calcinated eggshells

Compound	Composition (wt%)
CaO	89.3
SiO <sub>2</sub>	0.36
Fe <sub>2</sub> O <sub>3</sub>	0.02
MgO	1.16
SO <sub>3</sub>	0.23
K <sub>2</sub> O	0.04
Na <sub>2</sub> O	0.07
P <sub>2</sub> O <sub>5</sub>	0.48
TiO <sub>2</sub>	0.006
Mn <sub>2</sub> O <sub>3</sub>	0.004
Cr <sub>2</sub> O <sub>3</sub>	0.001
*LOI	9.71

\*LOI: Loss on ignition (CO<sub>2</sub>)

### 3.2 Physical characteristics of HAp from eggshells

The process of HAp synthesis from eggshell waste using urea and (NH<sub>4</sub>)<sub>2</sub>HPO<sub>4</sub> is dependent on the concentration of both materials. In a separate investigation conducted by Febriane [18], it was demonstrated that the addition of urea could regulate the pH gradually, resulting in HAp with a more homogeneous and uniform structure. Conversely, the addition of (NH<sub>4</sub>)<sub>2</sub>HPO<sub>4</sub> alters the physical properties of the resultant HAp. Higher concentrations of (NH<sub>4</sub>)<sub>2</sub>HPO<sub>4</sub> can yield HAp, which is purer white with a dense crystal structure, while lower concentrations of (NH<sub>4</sub>)<sub>2</sub>HPO<sub>4</sub> (0.5 M) produced HAp crystals that were yellowish in color and possessed an adhesive texture. Based on these findings, the concentrations of urea and (NH<sub>4</sub>)<sub>2</sub>HPO<sub>4</sub> were evaluated to determine the optimal conditions for the process.

The synthesized HAp product resulting from the reaction of calcium acetate with (NH<sub>4</sub>)<sub>2</sub>HPO<sub>4</sub> and urea exhibits different physical characteristics from its raw materials. As shown in Figure 1(a-c), each stage of the process, such as calcination

and synthesis, transforms the eggshell waste into various physical forms. This confirms that each step in the HAp formation process was successfully executed, producing distinct products at each stage. HAp typically appears as a white, milky powder. However, in some cases, the synthesized HAp may appear white-yellowish, which could indicate an issue with the synthesis process [19].

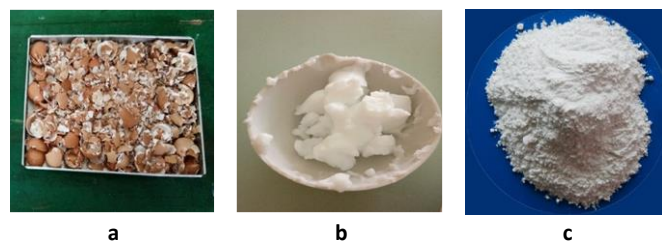


**Figure 1.** Physical characteristics of the HAp synthesis process: (a) raw eggshells before processing, (b) wet HAp precipitate after a 24-hour precipitation process (1.5 M), and (c) final HAp product after oven drying

### 3.3 Effects of urea and (NH<sub>4</sub>)<sub>2</sub>HPO<sub>4</sub> concentrations on HAp mass

It is essential to consider the impact of urea and (NH<sub>4</sub>)<sub>2</sub>HPO<sub>4</sub> concentration on the formation and properties of HAp. (NH<sub>4</sub>)<sub>2</sub>HPO<sub>4</sub> has been identified as a consolidant that promotes the formation of calcium phosphate, particularly HAp [20]. Studies have shown that adding (NH<sub>4</sub>)<sub>2</sub>HPO<sub>4</sub> to wet chemical precipitation methods leads to the precipitation of HAp along with other carbonated apatites [21]. Furthermore, research has explored the use of (NH<sub>4</sub>)<sub>2</sub>HPO<sub>4</sub> for strengthening materials like chalk, indicating its potential to enhance the properties of HAp [22].

Moreover, the concentration of reagents, including (NH<sub>4</sub>)<sub>2</sub>HPO<sub>4</sub> was highlighted as a crucial factor affecting the properties of HAp. Studies have demonstrated that the concentration of reagents, pH values, and other parameters significantly influence the morphology and properties of HAp [23]. Additionally, the impregnation of activated carbon fibers with (NH<sub>4</sub>)<sub>2</sub>HPO<sub>4</sub> has enhanced their performance for energy storage applications, suggesting a positive impact on material properties [24, 25]. The significance of observed morphological features such as agglomerations and pores is crucial for biomedical applications, particularly in orthopedic and dental fields. Agglomeration of particles influences the mechanical properties and bioactivity of HAp, impacting cell attachment and proliferation essential for bone regeneration. Porosity enhances biointegration and resorption rates by allowing cell infiltration and nutrient diffusion, which are key for bone tissue engineering. These features can be optimized to tailor HAp for specific biomedical uses, such as non-load-bearing applications or load-bearing implants.

The effects of urea and (NH<sub>4</sub>)<sub>2</sub>HPO<sub>4</sub> on the synthesis of HAp are shown in Figure 2. Pure urea solutions with different concentrations of 1, 1.5, and 2 M dissociated into NH<sub>3</sub> and CO<sub>2</sub>. NH<sub>3</sub> dissociates into NH<sub>4</sub><sup>+</sup> and OH<sup>-</sup> in water, whereas CO<sub>2</sub> forms CO<sub>3</sub><sup>2-</sup>. The NH<sub>3</sub> dissociated in water into NH<sub>4</sub><sup>+</sup> and OH<sup>-</sup> regulates the pH during the HAp synthesis reaction. The increased NH<sub>4</sub>OH formed is beneficial to the precipitation process during HAp synthesis. The solutions were preheated to change the pH from 6 to 9, resulting in NH<sub>3</sub> formation, which dissociates in water into NH<sub>4</sub>OH. Furthermore, heating the solution also causes CO<sub>2</sub> gas in the water to form CO<sub>3</sub><sup>2-</sup>.

$\text{CO}_3^{2-}$  will substitute into the HAp compound, replacing  $\text{PO}_4^{3-}$  ions.  $\text{CO}_3^{2-}$  substituted HAp has characteristics more suitable for human bone than stoichiometric HAp. Human bone has slight differences from stoichiometric HAp because human bone contains ions like  $\text{CO}_3^{2-}$ ,  $\text{Cl}^-$ ,  $\text{F}^-$ ,  $\text{Mg}^{2+}$ , and  $\text{Na}^+$ . Natural HAp in the human body contains 3-8% by weight carbonate. Three concentrations of  $(\text{NH}_4)_2\text{HPO}_4$  varied: 0.5, 1.0, and 1.5 M.  $(\text{NH}_4)_2\text{HPO}_4$  was used as a phosphate source. In addition to affecting the mass, the higher the concentration of  $(\text{NH}_4)_2\text{HPO}_4$ , the whiter and more solid the HAp crystals were obtained. At a concentration of 0.5 M  $(\text{NH}_4)_2\text{HPO}_4$ , the obtained HAp was slightly yellowish and somewhat sticky in crystal form (Figure 3). The observations in Figures 2 and 3 indicate that the HAp product obtained with 2.0 M urea and 1.5 M  $(\text{NH}_4)_2\text{HPO}_4$  is optimal. Therefore, the HAp characteristics analyzed pertain to the product derived from the precipitation reaction at these specific concentrations.

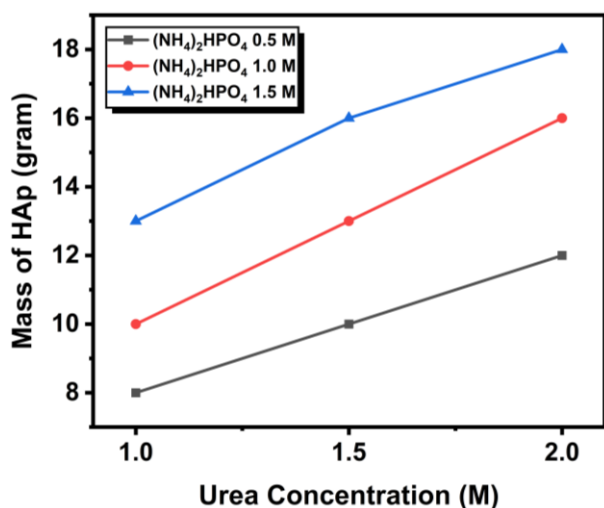


**Figure 2.** Different concentrations of urea and  $(\text{NH}_4)_2\text{HPO}_4$  influence the resulting HAp mass



**Figure 3.** The physical appearance of synthesized HAp with  $(\text{NH}_4)_2\text{HPO}_4$  concentrations of (a) 0.5 M, (b) 1.0 M, and (c) 1.5 M

Numerous studies have reported on the hydroxyapatite (HAp) synthesis processes utilizing various waste material sources. Comparative analyses were conducted to evaluate the characteristics of the HAp produced in this study relative to those from other investigations. Table 2 presents several studies pertaining to HAp synthesis.

**Table 2.** Comparison of HAp from various raw material sources

Waste Material Source	Method	Ca/P	Shape	Ref.
Clam shell	Methanochemical	1.6	Agglomerate polygonal	[26]
Sea shell	Precipitation with phosphoric acid	1.8	Rod-like	[27]
Mussel shell	Rapid Microwave irradiation with $\text{Na}_2\text{HPO}_4$	1.65	Rod-like	[28]
Egg shell	Precipitation	1.7	Globules	[29]
Egg shell	Precipitation with urea and $(\text{NH}_4)_2\text{HPO}_4$	1.23	Granular spherical	This study

### 3.4 Morphology and elemental analysis of HAp from eggshells

Analysis using SEM-EDX provides an overview of the morphology and atomic elements of the resulting HAp. The morphological observations of HAp derived from chicken eggshell waste can be seen in Figure 4. There are agglomerations and several granular non-uniform spherical HAp crystals. Based on the quantitative analysis of the morphology, the HAp crystals have observable pores with diameters ranging from 111.7 nm to 189.8 nm. Brahimi et al. [30] also reported the presence of agglomeration on the surface of the obtained HAp crystals, likely due to two biological integration processes, such as dissolution and subsequent precipitation.

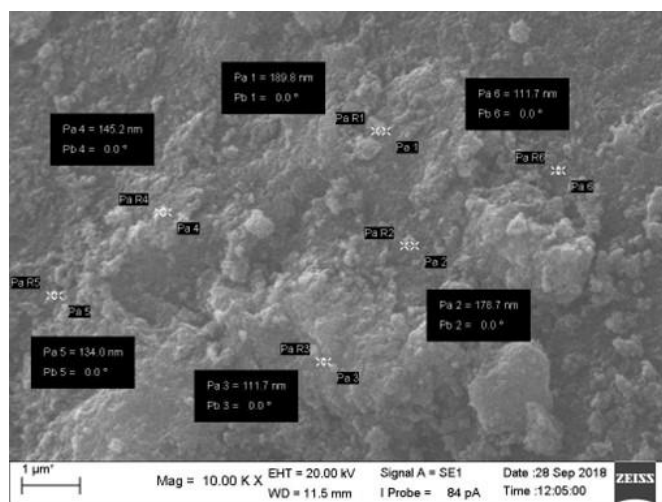


**Figure 4.** Morphology of HAp particles as observed by SEM at a magnification of 10,000

Based on the atomic elemental composition analysis shown in Table 3, the HAp produced from eggshell waste is predominantly composed of oxygen, phosphorus, and calcium, with respective values of 44.72, 16.74, and 26.61 wt%. Other elemental impurities are present in the HAp product with concentrations below 3 wt%. The presence of impurities in the product is likely due to incomplete elimination during the calcination process. In a study conducted by Tyszka-Czochara et al. [31], the EDX analysis of HAp showed atomic compositions of 39.9, 18.5, and 41.4 wt% for calcium, phosphorus, and oxygen, respectively. The

differences in these values compared to the results of this study are likely due to variations in synthesis processes and conditions. However, the HAp product in both studies is still predominantly composed of these three elements (calcium, oxygen, and phosphorus).

**Table 3.** EDX analysis of HAp from eggshells

Element	Series	Unn. C [wt. %]	Norm. C [wt. %]	Atom. C [wt. %]	(1 sigma) [wt. %]
Oxygen	K-series	44.72	44.01	67.37	6.99
Magnesium	K-series	0.39	0.39	0.40	0.07
Phosphorus	K-series	16.74	16.96	13.41	0.70
Calcium	K-series	26.61	26.96	16.47	0.85
Antimony	L-series	11.54	11.69	2.35	0.43
Total		100.00	100.00	100.00	

### 3.5 Functional group of HAp from eggshells

Fourier Transform Infrared Spectroscopy (FTIR) was used to characterize the functional groups of the obtained HAp. The spectrum shows the presence of OH<sup>-</sup>, PO<sub>4</sub><sup>3-</sup>, and CO<sub>3</sub><sup>2-</sup> groups (Figure 5). The phosphate group (PO<sub>4</sub><sup>3-</sup>) bond was the strongest, with stretching vibrations at 1000-1050 cm<sup>-1</sup> and medium intensity at 960 cm<sup>-1</sup>. Additionally, bending vibrations were observed at 560-610 cm<sup>-1</sup> [10]. The PO<sub>4</sub><sup>3-</sup> group exhibited the highest intensity at wavelengths of 567.07, 960.55, and 1043.49 cm<sup>-1</sup>. The OH<sup>-</sup> group, a constituent of Ca<sub>10</sub>(PO<sub>4</sub>)<sub>6</sub>(OH)<sub>2</sub>, formed at a wavelength of 3128.54 cm<sup>-1</sup>.

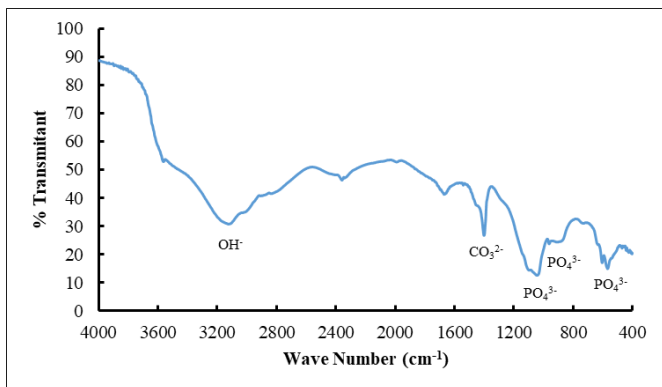


**Figure 5.** FTIR spectrum of obtained HAp from eggshells

The presence of carbonate groups (CO<sub>3</sub><sup>2-</sup>) (AKA and AKB) in the HAp structure has significant implications for its similarity to natural bone apatite. In natural bone, carbonate ions replace some phosphate (PO<sub>4</sub><sup>3-</sup>) and hydroxide (OH<sup>-</sup>) groups, forming A-type (carbonate substitution at OH sites), which occurs at high temperatures during precipitation, and B-type (carbonate substitution at PO<sub>4</sub><sup>3-</sup> sites) carbonate apatite, which occurs at low temperatures during precipitation. The carbonate in the sample was present at wavelengths between 1400-1460 cm<sup>-1</sup>, indicating it as AKB. This substitution reduces the crystallinity and increases the solubility of HAp, making it more biologically active and similar to the properties of natural bone mineral. Consequently, carbonate-substituted HAp can enhance the bioactivity, promote bone cell

attachment, and facilitate the integration with host bone tissue, making it more suitable for bone regeneration applications.

### 3.6 Crystallinity and crystal size analysis of HAp from eggshells

Based on the obtained XRD spectrum, quantitative calculations of the crystallinity and crystal size of HAp derived from eggshell waste can be performed. Eqs. (1) and (2) are used to calculate the percentage of crystallinity (*CrI*) and crystal size ( $\tau$ ), where  $I_{am}$  is the intensity of diffraction,  $I_{200}$  is the maximum intensity,  $k$  is a constant (0.89),  $\lambda$  is the wavelength of the incident beam,  $\beta$  is the full width at half maximum at Bragg's angle, and  $\theta$  is the angle between the incident ray and the scattering planes [28]. Figure 6 shows the HAp spectrum obtained from eggshells. The diffraction pattern values at  $2\theta$ , i.e., 26.111°, 32.252°, and 34.040°, exhibit the unique characteristics of HAp [32]. From the calculations performed, the crystallinity and crystal size of HAp were found to be 53.64% and 5.392 nm, respectively.

$$CrI = 1 - \frac{I_{am}}{I_{200}} \times 100\% \quad (1)$$

$$\tau = \frac{k\lambda}{\beta \cos\theta} \quad (2)$$

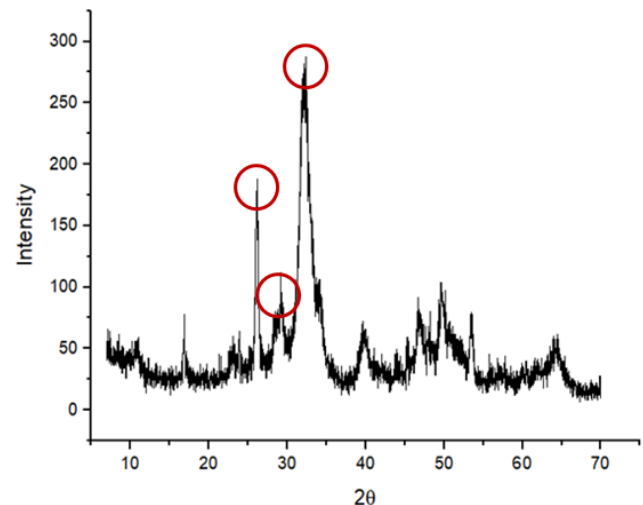


**Figure 6.** XRD pattern of obtained HAp

### 3.7 Thermal property of HAp from eggshells

The thermal analysis of HAp from eggshells was performed using DSC to measure the energy absorbed or emitted as a function of time or temperature. When thermal transitions occur in HAp, DSC provides calorimetric measurements of the transition energy at a given temperature. Figure 7 shows the relationship between the increase in temperature and the indication of the degradation of substances within the HAp material from eggshells. The endothermic peak at 95°C indicates the dehydration process of H<sub>2</sub>O molecules on the surface of HAp. Satish et al. [32] reported in their study that HAp derived from kaolin exhibits an endothermic peak at 80°C, corresponding to the removal of adsorbed water. At 204.12°C, a broad endothermic peak indicates the glass transition temperature of HAp. Meanwhile, at 385.68°C, a thermogram peak with exothermic enthalpy characteristics appears, indicating a crystallization process. At

this temperature, the crystal lattice structure of hydroxyapatite, initially amorphous, was formed.

At 617°C, hydroxyapatite undergoes decarbonization, followed by dehydroxylation at 813°C, both characterized by endothermic peaks. Chemically absorbed water requires more energy to be released from the structure during the dehydroxylation process, making it endothermic. During this process, hydroxyapatite is converted into calcium-deficient hydroxyapatite (CDHA) [33]. Gradual dehydroxylation at temperatures above 900°C leads to the decomposition of CDHA into  $\beta$ -tricalcium phosphate [34]. The melting point of hydroxyapatite is estimated to be above 1100°C.

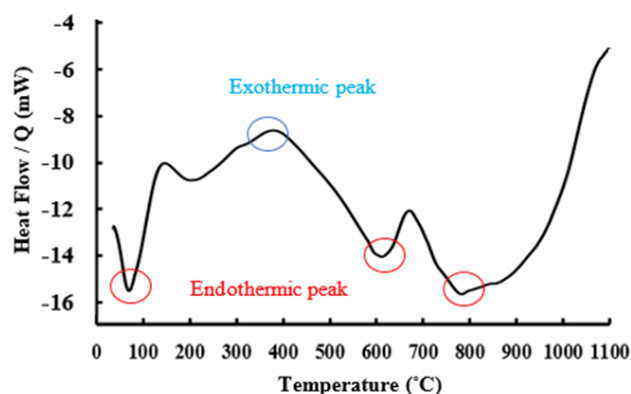


**Figure 7.** Correlation of heat flow vs temperature from DSC analysis of obtained HAp

#### 4. CONCLUSIONS

This study successfully synthesized carbonate-substituted HAp from urea and  $(\text{NH}_4)_2\text{HPO}_4$  using chicken eggshell waste as the calcium source. The findings demonstrate that varying concentrations of urea and  $(\text{NH}_4)_2\text{HPO}_4$  significantly impact the mass yield, crystal structure, and physical properties of the resulting HAp. The FTIR analysis confirmed the presence of functional groups characteristic of HAp, including  $\text{OH}^-$ ,  $\text{PO}_4^{3-}$ , and  $\text{CO}_3^{2-}$  groups. SEM observations revealed that the synthesized HAp has a granular form with non-uniform shapes and sizes, with particle diameters ranging from 111.7 to 189.8 nm. XRD analysis indicated that the synthesized HAp had a crystallinity of 53.64% and an average crystal size of 5.392 nm. Thermal properties of the synthesized HAp were analyzed using DSC, which identified several thermal transitions, including dehydration, glass transition, and crystallization processes. The study concludes that chicken eggshells, a readily available and low-cost waste material, can effectively produce high-quality HAp, contributing to sustainable waste management and developing valuable bioceramic materials for biomedical applications. Utilizing eggshell waste as a sustainable calcium source not only reduces environmental pollution caused by discarded eggshells but also offers economic benefits by providing a cost-effective alternative to synthetic calcium sources. By repurposing this agricultural waste, the production of HAp becomes more environmentally friendly, aligning with global efforts toward sustainability and resource conservation. Future research should focus on optimizing the synthesis parameters and exploring the potential applications of the synthesized HAp in various biomedical fields, as well as in drug delivery systems, bone tissue engineering, and adsorption processes.

#### REFERENCES

- [1] Alam, M.K., Hossain, M.S., Kawsar, M., Bahadur, N.M., Ahmed, S. (2024). Synthesis of nano-hydroxyapatite using emulsion, pyrolysis, combustion, and sonochemical methods and biogenic sources: A review. *RSC Advances*, 14(5): 3548-3559. <https://doi.org/10.1039/D3RA07559A>
- [2] Agbeboh, N.I., Oladele, I.O., Daramola, O.O., Akinwekomi, A.D., Tanimola, M.O., Olasukanmi, O. (2022). Comparing the effects of two wet precipitation methods on the yield of chicken eggshell-derived hydroxyapatite. *Futa Journal of Engineering and Engineering Technology*, 16(1): 95-104. <https://doi.org/10.51459/futajcet.2022.16.1.350>
- [3] Qi, M.L., Wu, Y., Sun, C., Zhang, H., Yao, S. (2023). Citrate-assisted one-pot hydrothermal preparation of carbonated hydroxyapatite microspheres. *Crystals*, 13(4): 551. <https://doi.org/10.3390/cryst13040551>
- [4] Mendez-Lozano, N., Apátiga-Castro, M., Soto, K.M., Manzano-Ramírez, A., Zamora-Antuñano, M., Gonzalez-Gutierrez, C. (2022). Effect of temperature on crystallite size of hydroxyapatite powders obtained by wet precipitation process. *Journal of Saudi Chemical Society*, 26(4): 101513. <https://doi.org/10.1016/j.jscs.2022.101513>
- [5] Rosa, A.L., Farias, L.R., Dias, V.P., Pacheco, O.B., Morisso, F.D., Junior, L.F.R., Sagrillo, M.R., Rossato, A., Santos, L.A.L., Volkmer, T.M. (2022). Effect of synthesis temperature on crystallinity, morphology and cell viability of nanostructured hydroxyapatite via wet chemical precipitation method: Effect of temperature on hydroxyapatite properties. *International Journal of Advances in Medical Biotechnology-IJAMB*, 5(1): 29-35. <https://doi.org/10.52466/ijamb.v5i1.110>
- [6] Pu'Ad, N.M., Koshy, P., Abdullah, H.Z., Idris, M.I., Lee, T.C. (2019). Syntheses of hydroxyapatite from natural sources. *Heliyon*, 5(5): e01588. <https://doi.org/10.1016/j.heliyon.2019.e01588>
- [7] Oladele, I.O., Agbabiaka, O.G., Adediran, A.A., Akinwekomi, A.D., Balogun, A.O. (2019). Structural performance of poultry eggshell derived hydroxyapatite based high density polyethylene bio-composites. *Heliyon*, 5(10): e02552. <https://doi.org/10.1016/j.heliyon.2019.e02552>
- [8] Wanniarachchi, W.A., Janani, V., Sutharsini, U., Thanihachelvan, M., Ramesh, S., Ng, C.K. (2023). Synthesis and sintering studies of hydroxyapatite derived from biogenic waste materials. In 8th Brunei International Conference on Engineering and Technology, Bandar Seri Begawan, Brunei Darussalam. <https://doi.org/10.1063/5.0113860>
- [9] Gintu, A.R., Kristiani, E.B.E., Martono, Y. (2022). The synthesis and physicochemical characterization of hydroxyapatite (HAp) from local duck egg shells. *JKPK (Jurnal Kimia dan Pendidikan Kimia)*, 7(1): 86-97. <https://doi.org/10.20961/jkpk.v7i1.55429>
- [10] Wu, S.C., Hsu, H.C., Wang, H.F., Liou, S.P., Ho, W.F. (2023). Synthesis and characterization of nano-hydroxyapatite obtained from eggshell via the hydrothermal process and the precipitation method. *Molecules*, 28(13): 4926. <https://doi.org/10.3390/molecules28134926>
- [11] Azis, Y., Adrian, M., Alfariis, C.D., Khairat, Sri, R.M.

- (2018). Synthesis of hydroxyapatite nanoparticles from egg shells by sol-gel method. In 2nd International Conference on Oleo and Petrochemical Engineering (ICOOPChE 2017), Pekanbaru-Riau, Indonesia. <https://doi.org/10.1088/1757-899X/345/1/012040>
- [12] Yudin, A., Ilinykh, I., Chuprunov, K., Kolesnikov, E., Kuznetsov, D., Leybo, D., Godymchuk, A. (2019). Microwave treatment and pH influence on hydroxyapatite morphology and structure. In XV International Conference of Students and Young Scientists "Prospects of Fundamental Sciences Development", Tomsk, Russian Federation. <https://doi.org/10.1088/1742-6596/1145/1/012003>
- [13] Abdelmoaty, A., Mousa, S. (2024). Synthesis and characterization of hydroxyapatite nanoparticles from calcium hydroxide fouled with gases evolved from smokestack of glass industry. *Scientific Reports*, 14(1): 10969. <https://doi.org/10.1038/s41598-024-60970-2>
- [14] Nicoara, A.I., Voineagu, T.G., Alecu, A.E., Vasile, B.S., Maior, I., Cojocaru, A., Trusca, R., Popescu, R.C. (2023). Fabrication and characterisation of calcium sulphate hemihydrate enhanced with Zn-or B-doped hydroxyapatite nanoparticles for hard tissue restoration. *Nanomaterials*, 13(15): 2219. <https://doi.org/10.3390/nano13152219>
- [15] Khalid, M., Jikan, S.S., Adzila, S., Yunus, Z.M., Badarulzaman, N.A. (2022). Characterizations of calcium oxide from calcined eggshell waste. *Key Engineering Materials*, 908: 130-134. <https://doi.org/10.4028/p-s8ckr0>
- [16] Razak, A., Isa, N.M., Kinit, S., Adzila, S. (2023). Effect of Calcination temperature on the properties of eggshell waste (EW) powder for biomedical application. *Evergreen*, 10(2): 782-791. <https://doi.org/10.5109/6792828>
- [17] Eze, S.C., Yawas, D.S., Dauda, E.T. (2024). Effect of calcined eggshell particles on some properties and microstructure of Al-Si-Mg alloy. *Journal of Scientific Research*, 16(1): 1-16. <https://doi.org/10.3329/jsr.v16i1.62231>
- [18] Febriane, S. (2014). Pengaruh Penambahan Urea pada Proses Sintesis Senyawa. <http://repository.unand.ac.id/20021/3/judul.pdf>
- [19] Saeed, G.K., Essa, A.F., Said, S.A.A. (2020). Preparation and characterization of hydroxyapatite powder and study of hydroxyapatite-alumina Composite. In the Fifth International Scientific Conference of Al-Khwarizmi Society (FISCAS), Iraq. <https://doi.org/10.1088/1742-6596/1591/1/012006>
- [20] Murru, A., Fort, R. (2020). Diammonium hydrogen phosphate (DAP) as a consolidant in carbonate stones: Impact of application methods on effectiveness. *Journal of Cultural Heritage*, 42: 45-55. <https://doi.org/10.1016/j.culher.2019.09.003>
- [21] Itua, A.N., Oluwole, O.I., Rangappa, S.M., Siengchin, S. (2023). Synthesis and characterization of hydroxyapatite powder from cattle bone. *Journal of Chemical Technology and Metallurgy*, 58(6): 1080-1092. <https://doi.org/10.59957/jctm.v58i6.147>
- [22] Samarkin, Y., Amao, A.O., Aljawad, M.S., Borji, M., Scott, N., Altammar, M.J., Alruwaili, K.M. (2023). In-situ micro-CT scanning and compressive strength assessment of diammonium hydrogen phosphate (DAP) treated chalk. *Scientific Reports*, 13(1): 16806. <https://doi.org/10.1038/s41598-023-43609-6>
- [23] Szturner, P., Antosik, A., Pagacz, J., Tymowicz-Grzyb, P. (2023). Morphology control of hydroxyapatite as a potential reinforcement for orthopedic biomaterials: The hydrothermal process. *Crystals*, 13(5): 793. <https://doi.org/10.3390/cryst13050793>
- [24] Gavrilov, N., Breitenbach, S., Unterweger, C., Fürst, C., Pašti, I.A. (2023). Exploring the impact of DAHP impregnation on activated carbon fibers for efficient charge storage and selective O<sub>2</sub> reduction to peroxide. *C — Journal of Carbon Research*, 9(4): 105. <https://doi.org/10.3390/c9040105>
- [25] Breitenbach, S., Lumetzberger, A., Hobisch, M.A., Unterweger, C., Spirk, S., Stifter, D., Fürst, C., Hassel, A.W. (2020). Supercapacitor electrodes from viscose-based activated carbon fibers: Significant yield and performance improvement using diammonium hydrogen phosphate as impregnating agent. *C — Journal of Carbon Research*, 6(2): 17. <https://doi.org/10.3390/c6020017>
- [26] Pal, A., Maity, S., Chabri, S., Bera, S., Chowdhury, A.R., Das, M., Sinha, A. (2017). Mechanochemical synthesis of nanocrystalline hydroxyapatite from Mercenaria clam shells and phosphoric acid. *Biomedical Physics & Engineering Express*, 3(1): 015010. <https://doi.org/10.1088/2057-1976/aa54f5>
- [27] Santhosh, S., Prabu, S.B. (2013). Thermal stability of nano hydroxyapatite synthesized from sea shells through wet chemical synthesis. *Materials Letters*, 97: 121-124. <http://doi.org/10.1016/j.matlet.2013.01.081>
- [28] Shavandi, A., Bekhit, A.E.D.A., Ali, A., Sun, Z. (2015). Synthesis of nano-hydroxyapatite (nHA) from waste mussel shells using a rapid microwave method. *Materials Chemistry and Physics*, 149: 607-616. <http://doi.org/10.1016/j.matchemphys.2014.11.016>
- [29] Goloshchapov, D.L., Kashkarov, V.M., Rumyantseva, N.A., Seredin, P.V., Lenshin, A.S., Agapov, B.L., Domashevskaya, E.P. (2013). Synthesis of nanocrystalline hydroxyapatite by precipitation using hen's eggshell. *ceramics International*, 39(4): 4539-4549. <http://doi.org/10.1016/j.ceramint.2012.11.050>
- [30] Brahimi, S., Ressler, A., Boumchedda, K., Hamidouche, M., Kenzour, A., Djafar, R., Antunović, M., Bauer, L., Hvizdoš, P., Ivanković, H. (2022). Preparation and characterization of biocomposites based on chitosan and biomimetic hydroxyapatite derived from natural phosphate rocks. *Materials Chemistry and Physics*, 276: 125421. <https://doi.org/10.1016/j.matchemphys.2021.125421>
- [31] Tyszcza-Czochara, M., Suder, M., Dołhańczuk-Śródka, A., Rajfur, M., Rajfur, K., et al. (2022). Nature-inspired effects of naturally occurring trace element-doped hydroxyapatite combined with surface interactions of mineral-apatite single crystals on human fibroblast behavior. *International Journal of Molecular Sciences*, 23(2): 802. <https://doi.org/10.3390/ijms23020802>
- [32] Satish, P., Hadagalli, K., Praveen, L.L., Nowl, M.S., Seikh, A.H., Alnaser, I.A., Abdo, H.S., Mandal, S. (2023). Hydroxyapatite-clay composite for bone tissue engineering: Effective utilization of prawn exoskeleton biowaste. *Inorganics*, 11(11): 427. <https://doi.org/10.3390/inorganics11110427>
- [33] Lakrat, M., Jodati, H., Mejdoubi, E.M., Evis, Z. (2023). Synthesis and characterization of pure and Mg, Cu, Ag, and Sr doped calcium-deficient hydroxyapatite from

brushite as precursor using the dissolution-precipitation method. *Powder Technology*, 413: 118026. <https://doi.org/10.1016/j.powtec.2022.118026>

[34] Zyman, Z., Epple, M., Goncharenko, A., Tkachenko, M., Rokhmistrov, D., Sofronov, D., Orlov, H. (2023).

Reaction sintering in compacted hydrolysed carbonated calcium phosphate. *Processing and Application of Ceramics*, 17(4): 421-427. <https://doi.org/10.2298/PAC2304421Z>